

# Exact solutions in two-dimensional topological superconductors: Hubbard interaction induced spontaneous symmetry breaking

Motohiko Ezawa

Department of Applied Physics, University of Tokyo, Hongo 7-3-1, 113-8656, Japan

We present an exactly solvable model of a spin-triplet  $f$ -wave topological superconductor on the honeycomb lattice in the presence of the Hubbard interaction for arbitrary interaction strength. First we show that the Kane-Mele model with the corresponding spin-triplet  $f$ -wave superconducting pairings becomes a full-gap topological superconductor possessing the time-reversal symmetry. We then introduce the Hubbard interaction. The exactly solvable condition is found to be the emergence of perfect flat bands at zero energy. They generate infinitely many conserved quantities. It is intriguing that the Hubbard interaction breaks the time-reversal symmetry spontaneously. As a result, the system turns into a trivial superconductor. We demonstrate this topological property based on the topological number and by analyzing the edge state in nanoribbon geometry.

*Introduction:* Topological superconductors have been investigated intensively in this decade<sup>1,2</sup>. A particular feature is that they host Majorana fermions<sup>3-5</sup>. It is a crucial problem how the topological properties are affected by the presence of the interaction. It is in general a formidable task to attack this problem in strongly correlated systems. Nevertheless, if there are exactly solvable models, they are quite powerful since they provide us with a clear physical understanding. Exact solutions in one-dimensional Kitaev topological superconductors have been constructed<sup>6-10</sup>. On the other hand, as far as we are aware of, there are so far no exact solutions for higher dimensional topological superconductors.

A Kitaev spin liquid<sup>11</sup> on the honeycomb lattice is a beautiful example of the exact solvable model on interacting Majorana fermions. A key point is that two Majorana fermion operators are made C numbers on the basis of infinitely many conserved quantities present. Then the interacting Majorana fermion model is transformed into a free Majorana fermion model. It is recently shown that this method is also applicable to trivial BCS superconductors with the Hubbard interaction<sup>12</sup>. Explicit examples have been constructed for the square and cubic lattices.

In this paper, we investigate interacting two-dimensional topological superconductors on the honeycomb lattice. Our observation is that the exactly solvable condition is the emergence of perfect flat bands at zero energy. The operator degrees of freedom associated with the perfect flat bands become C-numbers, and generate infinitely many conserved quantities. The resultant Majorana fermion model is transformed into a free Majorana fermion model.

We explicitly analyze a Kane-Mele model with the spin-triplet  $f$ -wave superconductor, since the  $f$ -wave superconducting pairing is compatible with the honeycomb lattice structure [Fig.1]. We can tune this model so as to possess perfect flat bands at zero energy. The system becomes a full-gap superconductor. It is shown to be a time-reversal invariant topological superconductor by analytically evaluating the spin-Chern number. Next, we introduce the Hubbard interaction into this system. The system is still exactly solvable for arbitrary interaction strength. It is intriguing that the time-reversal symmetry is spontaneously broken by the choice of the ground state. This leads to the conclusion that the system becomes a trivial superconductor, which we confirm by

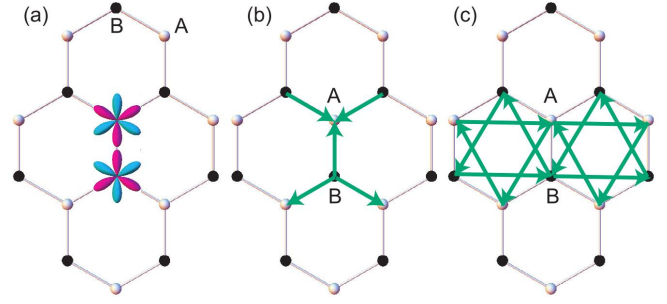


FIG. 1: (a) Illustration of the honeycomb lattice and the  $f$ -wave superconducting pairing. We see that the  $f$ -wave superconducting pairing is compatible with the honeycomb lattice. Superconducting pairings indicated by green arrows between (b) the nearest-neighbor sites and (c) the next-nearest neighbor sites. The sign is plus (minus) for the forward (backward) direction of the arrows. Arrows are pointing inside for A sites, while they are pointing outside for B sites in (b).

analyzing the edge states of zigzag nanoribbons.

*Model:* We start with the Kane-Mele model<sup>13</sup>  $H_{\text{KM}}$  on the honeycomb lattice with the spin-triplet  $f$ -wave superconducting pairing. As shown in Fig.1, the  $f$ -wave superconducting pairing is compatible with the honeycomb lattice and is natural as well as the  $s$ -wave superconducting pairing. We assume an equal spin pairing. The spin-triplet  $f$ -wave superconductors are realized by introducing the following interaction term<sup>14</sup>  $H_{\text{SC}}$ . We then introduce the Hubbard interaction  $H_{\text{Hubbard}}$ . The total Hamiltonian is given by

$$H = H_{\text{KM}} + H_{\text{SC}} + H_{\text{Hubbard}} \quad (1)$$

with

$$H_{\text{KM}} = -t \sum_{\langle i,j \rangle_s} c_{is}^\dagger c_{js} + i \frac{\lambda}{3\sqrt{3}} \sum_{\langle\langle i,j \rangle\rangle_s} \nu_{ij} \sigma_z c_{is}^\dagger c_{js}, \quad (2)$$

$$H_{\text{SC}} = -\Delta_1 \sum_{\langle i,j \rangle_s} c_{is}^\dagger c_{js}^\dagger + i \frac{\Delta_2}{3\sqrt{3}} \sum_{\langle\langle i,j \rangle\rangle_s} \nu_{ij} \sigma_z c_{is}^\dagger c_{js}^\dagger + \text{h.c.}, \quad (3)$$

$$H_{\text{Hubbard}} = U \sum_i \left( c_{i\uparrow}^\dagger c_{i\uparrow} - \frac{1}{2} \right) \left( c_{i\downarrow}^\dagger c_{i\downarrow} - \frac{1}{2} \right), \quad (4)$$

where  $c_{is}^\dagger$  creates an electron with spin polarization  $s$  at site  $i$ , and  $\langle i, j \rangle / \langle\langle i, j \rangle\rangle$  run over all the nearest/next-nearest neighbor hopping sites. We adopt the convention that  $s = \uparrow, \downarrow$  in indices and  $s = +1, -1$  in equations for the up and down spins. We explain each term: (i) The first term of the Hamiltonian  $H_{\text{KM}}$  represents the usual nearest-neighbor hopping with the transfer energy. (ii) The second term of the Hamiltonian  $H_{\text{KM}}$  represents the Kane-Mele spin-orbit coupling, where  $\sigma = (\sigma_x, \sigma_y, \sigma_z)$  is the Pauli matrix of spin, with  $\nu_{ij} = +1$  if the next-nearest-neighbor hopping is anticlockwise and  $\nu_{ij} = -1$  if it is clockwise with respect to the positive  $z$  axis. (iii) The first/second term of the Hamiltonian  $H_{\text{SC}}$  represents the nearest/next-nearest neighbor  $f$ -wave superconducting pairings. The system has the time-reversal symmetry.

*Non-interacting case:* First we investigate the non-interacting case;  $U = 0$ . The Hamiltonian is block diagonal with respect to the spin;  $H = H_\uparrow + H_\downarrow$ . In order to study superconductivity, we use the Bogoliubov de Gennes formalism. The honeycomb lattice is bipartite, which consists of the  $A$  and  $B$  sublattices. The nearest neighbor superconducting pairing occurs between the  $A$  and  $B$  sublattices, while the next-nearest neighbor superconducting pairing occurs within one sublattice: See Figs.1(b)–(c). The Nambu spinor consists of the electrons and holes, and reads  $\Psi_s = (c_{As}(k), c_{Bs}(k), c_{As}^\dagger(-k), c_{Bs}^\dagger(-k))$ . In the Nambu spinor basis the Hamiltonian  $H_s$  has the form

$$H_s = \begin{pmatrix} s\lambda S & tF & -s\Delta_2 S & \Delta_1 F \\ tF^* & -s\lambda S & -\Delta_1 F^* & -s\Delta_2 S \\ -s\Delta_2 S & -\Delta_1 F & s\lambda S & tF \\ \Delta_1 F^* & -s\Delta_2 S & -tF^* & -s\lambda S \end{pmatrix}, \quad (5)$$

with

$$F = e^{-iak_y/\sqrt{3}} + 2e^{iak_y/2\sqrt{3}} \cos \frac{ak_x}{2}, \quad (6)$$

$$S = \frac{2\lambda}{3\sqrt{3}} \left[ \sin ak_x - \sin \left( \frac{ak_x}{2} + \frac{\sqrt{3}ak_y}{2} \right) - \sin \left( \frac{ak_x}{2} - \frac{\sqrt{3}ak_y}{2} \right) \right]. \quad (7)$$

The eigenvalues read

$$E = \pm \sqrt{(t - \Delta_1)^2 |F|^2 + (\lambda - \Delta_2)^2 S^2}. \quad (8)$$

It is remarkable that perfect flat bands emerge when

$$\Delta_1 = t, \quad \Delta_2 = \lambda. \quad (9)$$

As we verify later, the emergence of perfect flat bands generates infinitely many conserved quantities and make one species of the Majorana fermions inactive in the theory with the interaction ( $U \neq 0$ ): See (21). In the following, we investigate the system by requiring this condition. When  $\lambda = 0$ , the gap closes linearly at the  $K$  and  $K'$  points. It is a Dirac nodal superconductor: See Fig.2(a). Once the  $\lambda$  becomes non-zero, the system becomes a full-gap superconductor: See Fig.2(d).

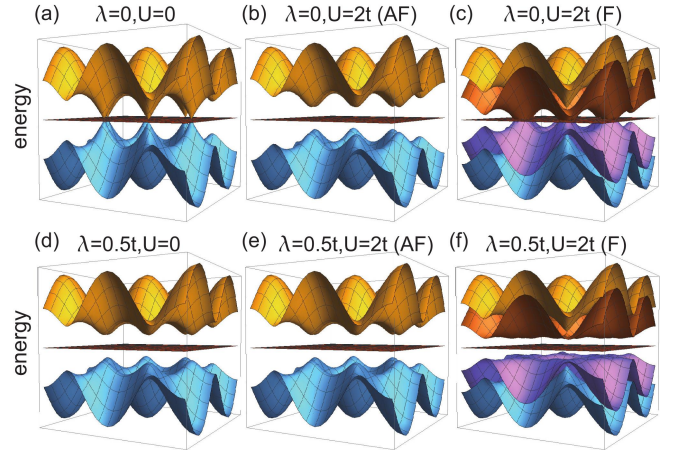


FIG. 2: Bird's eye's views of the bulk band structures on the  $k_x$ - $k_y$  plane, where (F) indicates the ferro-order, while (AF) indicates the antiferro-order. The energy of the antiferro-order is lower than that of the ferro-order. The vertical axis is the energy.

*Topological number:* We show that it is a topological superconductor by evaluating the topological numbers. They are the Chern number  $\mathcal{C}$  and the spin-Chern number  $\mathcal{C}_\sigma$ . The Chern number is zero,  $\mathcal{C} = 0$ , due to the time-reversal symmetry. The spin-Chern number  $\mathcal{C}_\sigma$  is given by  $\mathcal{C}_\sigma = (\mathcal{C}_\uparrow - \mathcal{C}_\downarrow) / 2$  in terms of the spin-dependent Chern number  $\mathcal{C}_s$  for each spin subsector<sup>15–18</sup>. We find that  $\mathcal{C}_\sigma$  is zero for the flat bands since the eigen functions are given by  $\Psi = (1, 0, 1, 0)$  and  $\Psi = (0, -1, 0, 1)$  for them. In order to evaluate  $\mathcal{C}_s$  for the valence band, we make a Taylor expansion

$$F = \hbar v_F (\xi k_x - i k_y), \quad S = \xi \lambda, \quad (10)$$

where  $v_F = \frac{\sqrt{3}}{2\hbar} at$  is the Fermi velocity and  $\xi = 1$  for the  $K$  point and  $\xi = -1$  for the  $K'$  point. The Berry curvature is calculated as

$$\Omega_s(\mathbf{k}) = \nabla \times \mathbf{a}(\mathbf{k}) = \frac{s\lambda}{2 \left( (\hbar v_F k)^2 + \lambda^2 \right)^{3/2}}, \quad (11)$$

with the Berry connection  $a_i(\mathbf{k}) = -i \langle \psi(\mathbf{k}) | \frac{\partial}{\partial k_i} | \psi(\mathbf{k}) \rangle$ . The  $\mathcal{C}_s$  is explicitly evaluated as

$$\mathcal{C}_s = \int \Omega_s(\mathbf{k}) d^2\mathbf{k} / (2\pi) = \text{sgn}(s\lambda) / 2, \quad (12)$$

and hence we obtain

$$\mathcal{C}_\sigma = \text{sgn}(\lambda), \quad (13)$$

by adding the contributions from the  $K$  and  $K'$  points. Consequently, the system is topological for  $\lambda \neq 0$ . We note that the  $\mathbb{Z}_2$  index is identical to the spin-Chern number provided that the time-reversal symmetry is present and that the spin is a good quantum number. We may explicitly confirm the Chern number,  $\mathcal{C} = \mathcal{C}_\uparrow + \mathcal{C}_\downarrow = 0$ , as required by the time-reversal symmetry.

*Interacting case:* It is in general a very hard task to solve the problem involving the Hubbard interaction  $H_{\text{Hubbard}}$ , since it is not a quadratic interaction. However, as we soon see, the Hubbard interaction can be rewritten in the quadratic form under the flat band condition (9).

We introduce Majorana fermion operators  $\eta$  and  $\gamma$  for each sublattice defined by

$$c_{is} = \eta_{is} + i\gamma_{is}, \quad c_{is}^\dagger = \eta_{is} - i\gamma_{is}, \quad (14)$$

$$c_{js} = \gamma_{js} + i\eta_{js}, \quad c_{js}^\dagger = \gamma_{js} - i\eta_{js}, \quad (15)$$

for fermions on  $i \in A$  and  $j \in B$  sublattices. The Hamiltonian (1) is rewritten in terms of these Majorana fermions as

$$H_M = H^{(1)} + H^{(2)} + H_{\text{Hubbard}} \quad (16)$$

with

$$H^{(1)} = 2i \sum_{\langle i,j \rangle_s} [(\Delta_1 + t)\gamma_{is}\gamma_{js} + (\Delta_1 - t)\eta_{is}\eta_{js}], \quad (17)$$

$$H^{(2)} = \frac{1}{6\sqrt{3}} \sum_{\langle\langle i,j \rangle\rangle_s} \nu_{ij}\sigma_z [(\Delta_2 + \lambda)\gamma_{is}\gamma_{js} + (\Delta_2 - \lambda)\eta_{is}\eta_{js}], \quad (18)$$

$$H_{\text{Hubbard}} = U \sum_i (2i\eta_{i\uparrow}\gamma_{i\uparrow}) (2i\eta_{i\downarrow}\gamma_{i\downarrow}). \quad (19)$$

The time-reversal symmetry  $\mathcal{T}$  acts as<sup>19</sup>

$$\mathcal{T}^{-1}i\eta_{i\uparrow}\eta_{i\downarrow}\mathcal{T} = -i\eta_{i\uparrow}\eta_{i\downarrow}, \quad \mathcal{T}^{-1}i\gamma_{i\uparrow}\gamma_{i\downarrow}\mathcal{T} = -i\gamma_{i\uparrow}\gamma_{i\downarrow}. \quad (20)$$

It is remarkable that the  $\eta$  Majorana fermions are decoupled from the Hamiltonians (17) and (18) by requiring the flat band condition (9). Furthermore, when we define  $D_i = 2i\eta_{i\uparrow}\eta_{i\downarrow}$ ,  $D_i$  commutes with the Hubbard interaction (19). Hence we obtain  $[D_i, H_M] = 0$  for all sites  $i$ , which implies that  $D_i$  becomes a C number. It is given by  $D_i = \pm 1/2$  by using the relation  $D_i^2 = 1/4$ . It is analogous to the honeycomb Kitaev spin liquid model<sup>11</sup>. Substituting  $D_i$  to (19), the Hubbard interaction term becomes quadratic in terms of the Majorana fermion operators and we obtain

$$H = 4it \sum_{\langle i,j \rangle_s} \gamma_{is}\gamma_{js} + \frac{i\lambda}{3\sqrt{3}} \sum_{\langle\langle i,j \rangle\rangle_s} \nu_{ij}\sigma_z \gamma_{is}\gamma_{js} - U \sum_i D_i (2i\gamma_{i\uparrow}\gamma_{i\downarrow}). \quad (21)$$

This Hamiltonian is exactly solvable for any fixed set of  $D_i$ , since it is quadratic in terms of the fermion operators  $\gamma$ . A set of  $D_i$  serves as infinitely many conserved quantities that make the system exactly solvable.

There are two possibilities in the choice of the ground state with respect to the  $\eta$  Majorana fermions. One is the ferro-order where the sign of  $D_i$  is the same between the two sublattices  $D_i = 1/2$ , while the other is the antiferro-order where the sign of  $D_i$  is opposite between the two sublattices  $D_i = (-1)^i/2$ . The  $D_i = 1/2$  and  $D_i = -1/2$  are related by

the interchange of  $U$  and  $-U$ . Consequently, the time-reversal symmetry is spontaneously broken by a particular choice of  $D_i$  for the ground state.

In the basis  $\Psi = (\Psi_\uparrow, \Psi_\downarrow)$ , the Hamiltonian is written in the form

$$H = \begin{pmatrix} H_\uparrow & H_U \\ H_U^* & H_\downarrow \end{pmatrix}, \quad (22)$$

with

$$H_U = \frac{iU}{4} \begin{pmatrix} 1 & 0 & -1 & 0 \\ 0 & \pm 1 & 0 & \pm 1 \\ -1 & 0 & 1 & 0 \\ 0 & \pm 1 & 0 & \pm 1 \end{pmatrix}, \quad (23)$$

where the sign is  $+$  for the ferro-order and  $-$  for the antiferro-order. For the ferro-order, the eigenenergy is given by

$$E^2 = (t|F| \pm U/4)^2 + \lambda^2 S^2, \quad (24)$$

and for the antiferro-order, it is given by

$$E^2 = t^2 |F|^2 + \lambda^2 S^2 + U^2/16, \quad (25)$$

where the spectrum is doubly degenerated.

By using the relation,

$$\begin{aligned} & 2\sqrt{t^2 |F|^2 + \lambda^2 S^2 + U^2/16} - \sum_{\pm} \sqrt{(t|F| \pm U/4)^2 + \lambda^2 S^2} \\ &= \frac{t^2 |F|^2}{(t^2 |F|^2 + \lambda^2 S^2)^{2/3}} \frac{U^2}{16} + O(U^4), \end{aligned} \quad (26)$$

we find that the antiferro-order is the ground state in the second order of  $U$ . Actually this is the case for arbitrary  $U$  by numerically evaluating the energies and comparing them. The gap closes for the ferro-order with  $\lambda = 0$ . The system is a loop-nodal superconductor: See Fig.2(c). On the other hand, the gap does not close for the ferro-order with  $\lambda \neq 0$  [see Fig.2(b)] and the antiferro-order with arbitrary  $\lambda$  [see Fig.2(e) and (f)]. The band gap is given by  $\sqrt{\lambda^2 + U^2/16}$  for the antiferro-order. In addition to the above bands, there are perfect flat bands at zero energy, which do not change at all by the inclusion of the Hubbard interaction. This is because the flat bands are solely associated with the  $\eta$  Majorana fermions, which are irrelevant to the Hubbard interaction consisting solely of the  $\gamma$  Majorana fermions.

The spin-Chern number  $\mathcal{C}_\sigma$  is no longer a good topological number once the Hubbard interaction is switched on and a particular choice of the ground state is made. Indeed, the time-reversal symmetry is broken due to the last term of Eq.(21) for a fixed value of  $D_i$  for  $i$ . The  $Z_2$  index is also ill defined since the time-reversal symmetry is spontaneously broken. On the other hand, the Chern number is well defined and remains to be zero ( $\mathcal{C} = 0$ ) even if the spin is no longer a good quantum number. We can check that the Chern numbers of the two valence bands are precisely cancelled. We expect that there are no other topological numbers in the present system. Then, the

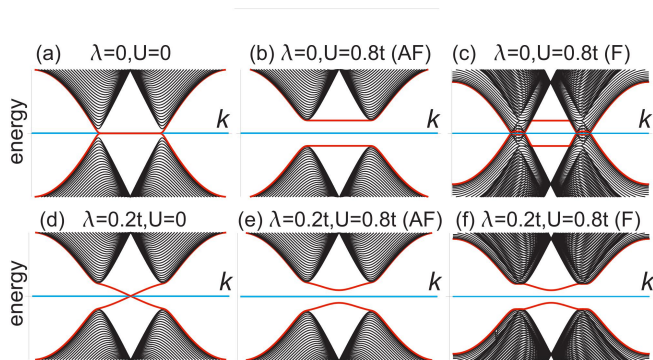


FIG. 3: The band structures of zigzag nanoribbons. The horizontal axis is the momentum  $k$  and the vertical axis is the energy. Perfect flat bands at zero energy are indicated by cyan, while the edge states are marked in magenta.

system turns into a trivial superconductor without gap closing due to the symmetry breaking<sup>20</sup>. It is possible to confirm this by calculating the edge states in nanoribbon geometry based on the bulk-edge correspondence.

*Edge states:* In order to verify whether the system is topological or not, we calculate the band structure for nanoribbon geometry. The band structure of nanoribbons is given in Fig.3. The band structures resemble those of graphene<sup>21</sup> for  $\lambda = 0$  [see Fig.3(a)] and silicene<sup>22</sup> for  $\lambda \neq 0$  [see Fig.3(d)] with the sole difference being the emergence of perfect flat bands at zero energy.

First, we investigate the case with  $\lambda = 0$ . There are partial flat bands connecting the  $K$  and  $K'$  points in addition to the perfect flat bands. These partial flat bands move away from zero energy once the interaction is introduced, as shown in Figs.3(b) and (c). The bulk spectrum is fully gapped for the antiferro-order [Fig.3(b)] and gapless for the ferro-order [Fig.3(c)] apart from the perfect flat bands.

Next, we investigate the case with  $\lambda \neq 0$ . When  $U = 0$ , there are helical edge states, as shown in Fig.3(d). These helical edge states anticross once the interaction is introduced for both the ferro-order [see Fig.3(f)] and the antiferro-order [see Fig.3(e)], which implies that the system turns into a trivial superconductor. This can be understood in the low-energy continuum theory. The helical edge states are perfectly localized in one of the sublattices. The low-energy Hamiltonian is effectively given by

$$H_{\text{edge}} = ivk[\gamma_{\uparrow}(k)\gamma_{\uparrow}(-k) - \gamma_{\downarrow}(k)\gamma_{\downarrow}(-k)] - iUD_i\gamma_{\uparrow}(k)\gamma_{\downarrow}(-k), \quad (27)$$

where  $v$  is the velocity of the helical edge. The eigenenergy reads

$$E = \pm\sqrt{v^2k^2 + U^2}, \quad (28)$$

which well describes the anticrossing of the helical edge states: See Figs.3(e) and (f). We note that the anticrossed edge states are almost the same between the ferro-order and the antiferro-order although the bulk spectrum is different, which implies the above low-energy theory is valid.

We have constructed exact solvable models on two-dimensional topological superconductors. The exact solvable condition is the emergence of perfect flat bands at zero energy, generating infinitely many conserved quantities and making one species of the Majorana fermions inactive. This method will be a guideline for searching further exact solvable models.

The author is very much grateful to N. Nagaosa for many helpful discussions on the subject. This work is supported by the Grants-in-Aid for Scientific Research from MEXT KAKENHI (Grant Nos.JP17K05490 and 15H05854). This work is also supported by CREST, JST (JPMJCR16F1).

<sup>1</sup> X.-L. Qi, S.-C. Zhang, Rev. Mod. Phys. 83, 1057-1110 (2011)

<sup>2</sup> M. Sato and Y. Ando, Rep. Prog. Phys. 80, 076501 (2017)

<sup>3</sup> J. Alicea, Rep. Prog. Phys. 75, 076501 (2012).

<sup>4</sup> C. W.J. Beenakker, Annu. Rev. Condens. Matter Phys. 4, 113 (2013).

<sup>5</sup> S.R. Elliott and M. Franz, Rev. Mod. Phys. 87, 137 (2015).

<sup>6</sup> H. Katsura, D. Schuricht, and M. Takahashi, Phys. Rev. B 92, 115137 (2015).

<sup>7</sup> J.-J. Miao, H.-K. Jin, F.-C. Zhang, and Y. Zhou, Phys. Rev. Letters 118, 267701 (2017).

<sup>8</sup> M. Ezawa, Phys. Rev. B 96, 121105(R) (2017)

<sup>9</sup> M. McGinley, J. Knolle, and A. Nunnenkamp, cond-mat/arXiv:1706.10249.

<sup>10</sup> Y. Wang, J.-J. Miao, H.-K. Jin, S. Chen, cond-mat/arXiv:1707.08430

<sup>11</sup> A. Kitaev, Annals of Physics 321, 2 (2006)

<sup>12</sup> Z. Chen, X. Li, and T. K. Ng, cond-mat/arXiv:1709.08411

<sup>13</sup> C. L. Kane and E. J. Mele, Phys. Rev. Lett. 95, 226801 (2005); ibid 95, 146802 (2005).

<sup>14</sup> L.-Y. Xiao, S.-L. Yu, W. Wang, Z.-J. Yao and J.-X. Li, EPL 115, 27008 (2016)

<sup>15</sup> L. Sheng, D. N. Sheng, C. S. Ting, and F. D. M. Haldane, Phys. Rev. Lett. 95, 136602 (2005)

<sup>16</sup> D. N. Sheng, Z. Y. Weng, L. Sheng and F. D. M. Haldane, Phys. Rev. Lett. 97 036808 (2006)

<sup>17</sup> Y. Yang, Z. Xu, L. Sheng, B. Wang, D.Y. Xing, and D. N. Sheng, Phys. Rev. Lett. 107, 066602 (2011)

<sup>18</sup> M. Ezawa, J. Phys. Soc. Jpn. 84, 121003 (2015)

<sup>19</sup> X.-L. Qi, T. L. Hughes, S. Raghu, and S.-C. Zhang

<sup>20</sup> M. Ezawa, Y. Tanaka and N. Nagaosa, Scientific Reports 3, 2790 (2013)

<sup>21</sup> M. Ezawa, Physical Review B, 73, 045432 (2006)

<sup>22</sup> M. Ezawa, New J. Phys. 14, 033003 (2012)